17

Multiscale Modelling of Solid Tumour Growth

Helen M. Byrne,[1] I.M.M. van Leeuwen,[1,2] Markus R. Owen,[1] Tomás Alarcón,[3] and Philip K. Maini[4]

[1] Centre for Mathematical Medicine and Biology, School of Mathematical Sciences, University of Nottingham, Nottingham NG7 2RD, UK
helen.byrne@nottingham.ac.uk, markus.owen@nottingham.ac.uk

[2] Department of Surgery and Molecular Oncology, Ninewells Hospital, University of Dundee, Dundee DD1 9SY, Scotland, UK
ingeborg@maths.dundee.ac.uk

[3] Department of Mathematics, Imperial College, 180 Queen's Gate, London SW7 2AZ, UK
a.tomas@imperial.ac.uk

[4] Centre for Mathematical Biology, Mathematical Institute, University of Oxford, 24-29 St Giles', Oxford OX1 3LB, and Oxford Centre for Integrative Systems Biology, Department of Biochemistry, South Parks Road, Oxford OX1 3QU, UK
maini@maths.ox.ac.uk

17.1 Introduction

Biological function arises from complex processes interacting over a large range of spatial and temporal scales. For example, within vascularised tumours, local oxygen levels, determined at the tissue scale by vascular density and blood flow, influence subcellular processes that include progress through the cell cycle and the expression of proteins such as vascular endothelial growth factor (VEGF). Since VEGF is a potent angiogenic factor, its intracellular production, release by the cells and transport through the extracellular space stimulate vascular adaptation at the macroscale. This remodelling, in turn, controls oxygen delivery to the tissue.

Over recent decades, remarkable technological advances within the life sciences have led to the generation of an enormous amount of data relating to phenomena that act at different scales. However, the impressive scientific contributions contained within individual articles are often fragmented and isolated due to the absence of comprehensive conceptual frameworks that allow information to be organised and results integrated. Furthermore, intuitive, verbal reasoning approaches can be inadequate for dealing with such complicated, non-linear dynamical systems. Nor can they keep pace with the vast amount of information being generated. Experience within other areas of science has taught us that quantitative methods are needed to develop com-

N. Bellomo et al. (eds.), *Selected Topics in Cancer Modeling*,
DOI: 10.1007/978-0-8176-4713-1_17,

prehensive theoretical models for interpretation, organisation and integration of these data [GM03].

The challenge for mathematical biology is two-fold: first to develop meaningful mathematical models at each individual scale, then to integrate such models into a computationally tractable multiscale model that allows us to understand how individual processes (for example, binding of a drug to its receptor) at the microscopic level affect the behaviour at the system (macroscopic) level (for example, the effect of a drug on a specific organ).

In addressing this challenge, modelling has two possible roles to play. First, on those rare occasions for which the biological system of interest has been well studied and characterised, it is possible to develop, with a fine degree of accuracy, models capable of replicating the biological observations. Whereas this is of little interest *per se*, exploiting the models to study the effect of different interventions can greatly enhance our understanding of the system's properties and behaviour. Hence, *in silico* techniques provide tools to carry out and iterate experiments that would otherwise be classified as unethical, expensive, time consuming, or simply impossible. Second, most research in biological systems is at a stage where it is impossible to develop accurate, detailed mathematical models. In these cases, modelling also has a vital role to play. Mathematical models essentially translate empirical biological hypotheses into a concrete framework which allows us to compute the outcome of these proposed interactions. By testing against data, this allows hypotheses to be verified or rejected and new hypotheses to be generated. This continual interaction between theoretical and empirical efforts makes it possible to refine the experimental procedure and leads to greater understanding of the complex system. Additionally, it should reduce the need for experimentation.

To exploit the full potential of mathematical modelling in biology, there is an urgent need to develop new theoretical tools for the analysis and synthesis of detailed low-level information into comprehensive, integrative, and quantitative descriptions that span a wide range of spatio-temporal scales. This new research area is viewed as the next "grand challenge" in the life sciences, and is often referred to as the Physiome Project,[5] encompassing the world-wide effort to describe biological function, based on genomic and proteomic mechanisms and their interaction, using qualitative and quantitative mathematical models [Cram04]. The ultimate goal is to transform the wealth of data being generated into a detailed understanding of biological function and, hence, of the complex systems that together form the basis of living organisms.

Within this effort, there is a growing literature devoted to mathematical modelling of different aspects of tumour growth (see, for example, the reviews in [Ad96, AMcE, RCM07]). These models tend to concentrate on processes occurring at one particular scale. Biologists now believe that the complexities of cancer could be explained in terms of a small number of underlying principles, namely, self-sufficiency in growth signals, insensitivity to anti-growth signals,

[5] http://www.physiome.org/

evasion of programmed cell death (apoptosis), limitless replication potential, sustained angiogenesis, tissue invasion and metastasis [HW00]. Our long-term goal is to incorporate these features into a multiscale "virtual tumour" model allowing us to organise existing data into an integrative theoretical framework that can clarify the underlying dynamics governing invasive cancers, and lead to the development of therapeutic strategies to combat tumour growth. However, in the shorter term, we can focus on certain aspects of cancer which are already amenable to experimental manipulation with a view to developing clinical strategies to control the disease. Our approach is to develop a multiscale model which can integrate existing models, extending them where appropriate, and be consistently updated by new experimental information. This requires the development of a theoretical framework into which models can be slotted as modules. We anticipate that the resulting model will be similar in scope to the heart models that have been developed by Noble, Hunter and co-workers [Cram04, Nobl06].

By way of illustration we present below three examples of our recent work. In Section 17.2, we present a model for carcinogenesis during the early (avascular) stages of ductal carcinoma *in situ* which focuses on aspects of metabolic changes and somatic evolution. In Section 17.3, we introduce a multiscale model for a vascularised tumour in which the dynamics of the tumour mass are intimately related to those of the blood vessels supplying the tissue with nutrients, and in Section 17.4 we present a model for early colorectal cancer. The common theme underlying these models is the integration of processes occurring on very different spatial and temporal scales. The chapter concludes in Section 17.5 with a summary of our results, a review of related relevant work and a discussion of the challenges that lie ahead for the further development of multiscale models of solid tumour growth in particular and their wider application in biology.

17.2 Metabolic Changes During Carcinogenesis

The pioneering work of Warburg [W30] revealed that tumour cells show an abnormal metabolism, preferentially converting glucose to lactic acid, even in the presence of sufficient oxygen. This is a paradox given that the aerobic glucose metabolic pathway is substantially more energy efficient than anaerobic metabolism, or glycolysis. It also has important clinical implications since a direct correlation between the rate of glucose consumption and tumour aggressiveness has been observed [HSR91]. The reason for this metabolic transition is as yet unclear. It has been proposed that, through factors such as cellular crowding, tumour cells may destroy the native vasculature, the primary mode of oxygen delivery, leading to heterogeneous oxygen perfusion through the tumour tissue. The resulting cyclical periods of hypoxia can initially cause transient adoption of glycolysis. However, the universal adoption of increased

glycolysis in human cancer, even under normal conditions, suggests that environmental factors other than hypoxia are involved.

We might expect that the increased acid production associated with the glycolytic phenotype would give rise to a significantly lower intracellular pH. However, magnetic resonance spectroscopy has shown that intracellular tumour pH is higher than that in non-transformed cells [GLB94]. This is due to upregulation of ion transporters which increase the flux of hydrogen ions across the tumour cell membrane into the extracellular space [GRM89]. A combination of this acid transport and the poor tumour vasculature for excess acid removal results in a tumour extracellular pH substantially lower than that of normal tissue. This has led to the acid-mediated tumour invasion hypothesis [GG96].

As the tumour microenvironment becomes more toxic, adaptation becomes essential. Recently a hybrid cellular automaton model has been developed to investigate the cell-microenvironmental interactions that mediate somatic evolution of cancer cells [SGGMG07] during the development of ductal carcinoma *in situ*. We briefly describe the model here, and refer the interested reader to the original paper for full details.

17.2.1 Model Framework

The model builds heavily on work by Gatenby and Gillies [GG04] who hypothesise that evolution of glycolysis is due to environmental constraints imposed by the morphology of the ducts. The blood supply is separated from the interior of the ducts by the basement membrane, so as a pre-malignant lesion grows away from the membrane into the duct it eventually experiences hypoxia. Gatenby and Gillies propose that this leads to an evolutionary sequence consisting of adaptation to hypoxia by upregulation of glycolysis, acidification of the environment (due to anaerobic respiration of glucose) and then cellular adaptation to acid-induced cellular toxicity.

The hybrid cellular automaton model that is used is composed of an (M $\times$ N) array of automaton elements (i, j) with a specific rule set governing their evolution. The distribution of the oxygen, glucose and H^+ fields is also monitored, reaction-diffusion equations being used to characterise their spatio-temporal dynamics. Each automaton element corresponds to a region of size 25μm $\times 25\mu$m that is occupied by either a tumour cell or a vacant space. Cells are initially placed as automaton units on the x-axis (the duct membrane). As they divide and undergo genetic alterations, cells move into the duct lumen. Nutrient levels are assumed to be in equilibrium, a reasonable assumption given the time scales associated with cell division, diffusion and their uptake by cells. Cells, in turn, metabolise nutrient into ATP. They are assumed to die if the ATP levels are below a certain threshold; otherwise they divide with a probability that depends on the "excess" amount of ATP. At each division cells can mutate into a different state (*i.e.* hyperplastic, glycolytic, acid-resistant) with a certain probability. During periods of

hypoxia, cells revert to anaerobic metabolism, producing lactic acid which is again modelled by a reaction-diffusion equation at equilibrium. This acid can cause cell death, depending on its concentration and the evolutionary state of the cell.

17.2.2 Simulation Results

Results from a typical simulation are presented in Fig. 17.1. The dynamics are, broadly speaking, consistent with those predicted in the verbal model of Gatenby and Gillies [GG04]. First, the hyperplastic cell type predominates, allowing cells to move away from the basement membrane into the duct lumen. Then, as hypoxia becomes important, the glycolytic cell type takes over, creating a highly acidic environment which eventually favours the acid-resistant cell type. However, the model predicts an extra feature, namely the possibility of long-lived transient islands of glycolytic cells surviving in a "sea" of acid-resistant cells. Motivated by this prediction, recent experiments have been carried out which do indeed verify this result [GS07]. The model is currently being extended to include more detailed aspects of the glycolytic pathway, and to investigate how the evolutionary process taking place within the duct may affect the invasiveness of the cell population which eventually breaks through the basement membrane.

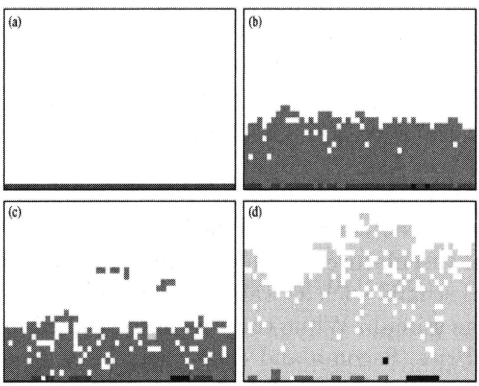

Fig. 17.1. The temporal evolution of a typical cellular automaton at (a) $t = 0$, (b) $t = 100$, (c) $t = 250$ and (d) $t = 300$ generations. Shown are normal epithelial (dark grey), hyperplastic (pink/grey), hyperplastic-glycolytic (green/grey) and hyperplastic-glycolytic-acid resistant (yellow/light grey) cells (colour version online). Cells with other phenotypic patterns are shown as black. Reproduced with permission from [SGGMG07].

17.3 Vascular Tumour Growth

Tumour tissue shares a complex relationship with vasculature. As a growing solid tumour reaches the limits of nutrient diffusion it is believed to secrete tumour angiogenesis factors (TAFs) to promote vascular growth towards and within the tumour. The new vasculature acts as a nutrient supply source and a (toxic) waste product disposal system, and provides access to distant parts of the body via metastatic invasion. At the same time, it allows the host to intensify its immunological response to the tumour cells through, for example, macrophages and neutrophils. As the access to increased nutrient availability allows the tumour to grow, the enhanced pressure of the tumour cells may cause the immature tumour vasculature to collapse [Jain88], creating areas of hypoxia which, in turn, stimulate the cells to secrete TAFs which widen existing blood vessels and create more new vessels. As we illustrate below, an understanding of such complex interactions can be facilitated by formulating, analysing and exploiting multiscale mathematical models.

17.3.1 Model Framework

The modelling framework is outlined in Fig. 17.2 which shows the spatial scales of interest (*e.g.* subcellular, cellular and tissue) and how the processes acting at the different scales interact. As in the model discussed in Section 17.2, nutrients and chemical signals are modelled using reaction-diffusion equations, and cells are modelled as automaton units. While cells can, as in the previous model, be considered as "black boxes" with prescribed parameters, cell properties (*e.g.* proteins associated with the cell cycle) can now be determined by ordinary differential equation (ODE) models operating on the intracellular scale.

The key advances in this model are the consideration of blood flow and vascular adaptation and their coupling to the dynamics of the tumour mass. It is known that normal vasculature is highly dynamic, with vessel radii responding to local mechanical stimuli such as wall shear stress, various biochemical stimuli and longer range stimuli. While this has been studied in great detail in the rat mesentery by Pries, Secomb and co-workers (see, for example, [PSG98]), only recently have similar models been advanced for tumours. In a series of papers, McDougall and co-workers have developed a hybrid model for vascular adaptation, blood flow and angiogenesis in which the tumour is viewed as a fixed source of angiogenic factors that does not grow [MACS02, MAC06]. By adapting an earlier discrete model of angiogenesis due to Anderson and Chaplain [AC98], endothelial cells within a capillary tip are assumed to perform random walks, biased by chemotaxis in response to tumour-derived angiogenic factors and haptotaxis in response to fibronectin gradients generated in the extracellular matrix through which the endothelial cells migrate. McDougall *et al.* used their model to highlight two important phenomena that could be responsible for the failure of blood-borne chemotherapy. First, most

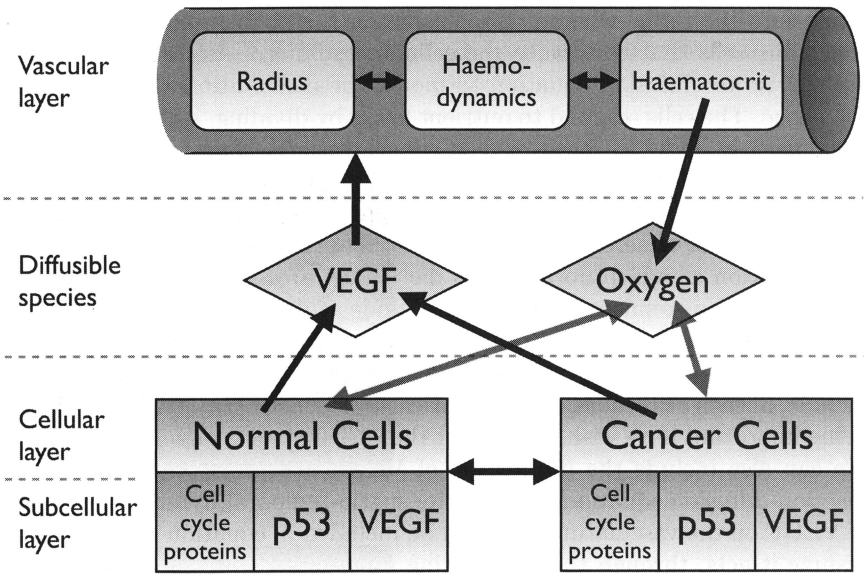

Fig. 17.2. Schematic diagram showing the structure of our multiscale model of vascular tumour growth.

of the drug may be diverted from the tumour by its highly interconnected capillary network. Second, dilution effects as the drug disperses through the vasculature may mean that the concentration reaching the tumour is too low to be effective. Further simulations suggested that increasing the mean radius of capillary vessels and/or decreasing the blood viscosity could substantially increase drug uptake.

In the absence of a detailed flow model for tumour vasculature, we take Pries *et al.*'s model and adapt it to tumours in a reasonable way. The model takes the form

$$R(t + dt) = R(t) + R(t)U(t)\, dt, \tag{17.1}$$

where $R(t)$ is the radius of a blood vessel at time t and dt is the time step. The remodelling function $U(t)$ consists of a number of components, as described above (for details, see [ABM05a, ABM05b, BAOMM]).

For simplicity, we consider a vascular network composed of a regular hexagonal array, with one input and one output, and a pressure drop imposed across it. We use the Poiseuille approximation and Kirchhoff's laws to compute the flow rates through and pressure drops across each vessel. Following [F93], we assume that at branch points the haematocrit, the red blood cells carrying oxygen, splits in proportion to the flow velocities in the daughter vessels. In this way, we can, in a simple first pass, compute the wall shear stresses and metabolic stimuli in each vessel and update their radii using equation (17.1) [ABM05b]. We assume that oxygen (nutrient) diffuses out of the vascu-

lature into the tissue where it is available for metabolism by the normal and cancerous cells that constitute the cellular automata. As in Section 17.2 we use a reaction-diffusion equation to model the distribution of oxygen within the tissue. The cells respond to nutrient levels by dividing, if the concentration is sufficiently high. At lower oxygen concentrations, cancerous cells can survive for a certain period of time by becoming quiescent, but normal cells die. We can phenomenologically take into account the effect of acid production as a by-product of anaerobic metabolism by lowering the threshold of nutrient concentration at which normal cells die if they are surrounded by cancerous cells (an obvious refinement will be to include acid explicitly as a field variable and to model the metabolic biochemistry in more detail [JPCF]).

The basic model can be extended in many ways. For example, we can include, in each cell, equations that caricature the cell cycle [TN01], such detail being important if we wish to consider the effect of cell-cycle-dependent drugs. We can also include the production of VEGF in hypoxic regions and use a reaction-diffusion equation to model its spatio-temporal dynamics. The effect of VEGF on the vasculature can then be included in equation (17.1) where we assume it acts, through the remodelling function $U(t)$, to increase the vessel radius (in effect we are modelling angiogenesis implicitly, an increase in the simulated vessel radius being taken to represent an increase in the number of vessels present in a particular tissue region).

Cell crowding can be included by associating with each element in the automaton a carrying capacity whose value may depend on the number of vessels, tumour cells and normal cells contained within a particular element, to reflect the physical differences between vessels and cells, and the different responses to contact inhibition from normal cells and tumour cells. Cell movement is modelled as a stochastic process, with transition probabilities depending on the space available at neighbouring sites [BAOMM].

17.3.2 Simulation Results

We now summarise some of the key results that we have obtained using our multiscale model of vascular tumour growth.

Haematocrit distribution influences tumour growth

The simulations presented in Fig. 17.3 illustrate the importance of accurately modelling blood flow through the tissue [ABM05a]. In both cases the vascular dynamics are independent of the tumour, but the cellular dynamics are influenced, via oxygen, by behaviour at the macroscale. The upper panels correspond to a case for which the vessels undergo structural adaptation and, hence, the haematocrit and oxygen are distributed non-uniformly across the tissue. The lower panels show how the system evolves when the haematocrit is distributed uniformly throughout the vessels (*i.e.* blood flow is identical in all branches of the vasculature). We see that spatial heterogeneity has a significant effect on the tumour's dynamics and, in this case, actually reduces the

tumour burden. We note also that when the oxygen distribution is heterogeneous the tumour develops "finger-like" protrusions similar to those observed in invasive cancers. Here this structure arises because the nutrient distribution is non-uniform.

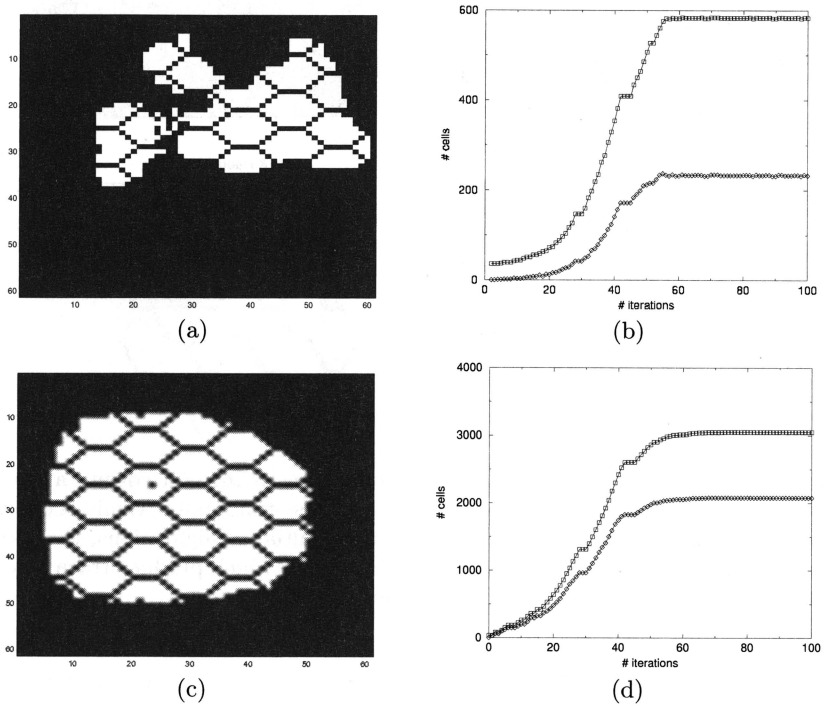

Fig. 17.3. Series of images showing the spatial distribution of cells for growth in inhomogeneous (panel a), and homogeneous environments (panel c). In panels (a) and (c) cancer cells occupy white spaces and vessels occupy a hexagonal array denoted by black spaces. The other black spaces denote empty spaces. Panels (b) and (d) show the time evolution of the number of (cancer) cells for the heterogeneous and homogeneous cases, respectively: squares denote the total number of cancer cells (proliferating + quiescent); diamonds denote quiescent cells. Reproduced with permission from [ABM03].

VEGF-dependent remodelling may stimulate oscillatory tumour dynamics

The simulation presented in Figs. 17.4 through 17.6 shows how coupling intracellular and macroscale phenomena can influence the dynamics of both the vasculature and the tumour [BAOMM]. In contrast to the results depicted in Fig. 17.3, where vessel adaptation was independent of VEGF, in Figs. 17.4 through 17.6 it is regulated by local VEGF levels. Figs. 17.4 and 17.5 show

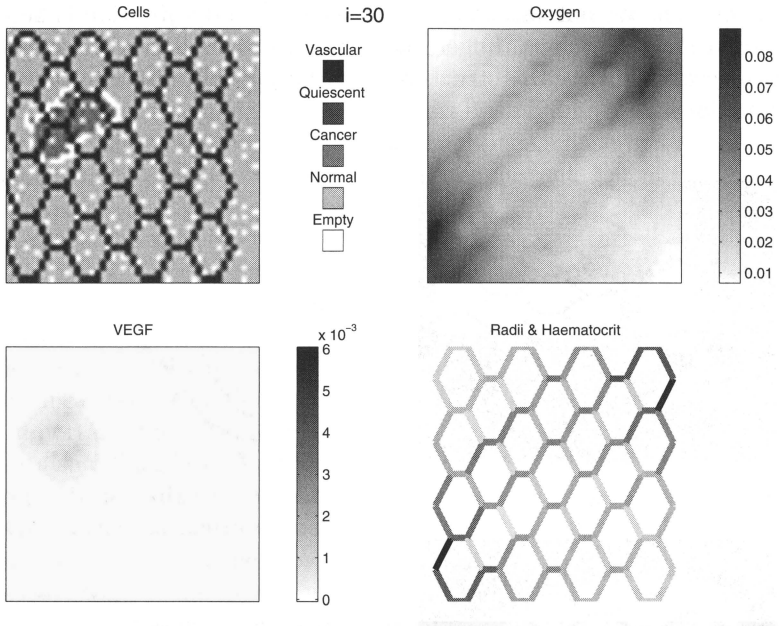

Fig. 17.4. Series of plots showing how a small tumour introduced into a vascular tissue at $t = 0$ has evolved at $t = 30$ (dimensionless time unit). While the oxygen and vessel profiles remain unchanged from their initial configurations, the tumour has increased in size and now contains quiescent cells which produce trace amounts of VEGF. Reproduced with permission from [BAOMM].

how the tumour's spatial composition evolves while Fig. 17.6 summarises its dynamics. Since there is a single inlet (outlet) to the vasculature located in the bottom left (top right) hand corner of the tissue, the incoming blood flow and haematocrit become diluted as they pass through the hexagonal lattice. This creates a heterogeneous oxygen distribution across the domain, with oxygen levels being highest near the inlet and outlet. Over time, the tumour cells proliferate and spread through the tissue towards oxygen-rich regions. As they increase in number, their demand for oxygen outstrips that available from the vasculature, and quiescent regions form. Cells in the quiescent regions produce VEGF which diffuses through the tissue (see Figs. 17.4 and 17.5), stimulating vessel adaptation and biasing blood flow towards low oxygen regions. If the VEGF stimulus is weak then the vasculature does not adapt quickly enough and the quiescent cells die (this is what happens at early times in Fig. 17.6). VEGF levels also decline and blood flow to the remaining tumour cells rises, enabling them to increase in number until the demand for oxygen once again exceeds that being supplied, and so the cycle repeats, with pronounced oscillations in the number of quiescent cells (see Fig. 17.6). In order to highlight the key role played by VEGF in creating these oscillations, also presented in Fig. 17.6 are the results of a simulation which was identical in all respects ex-

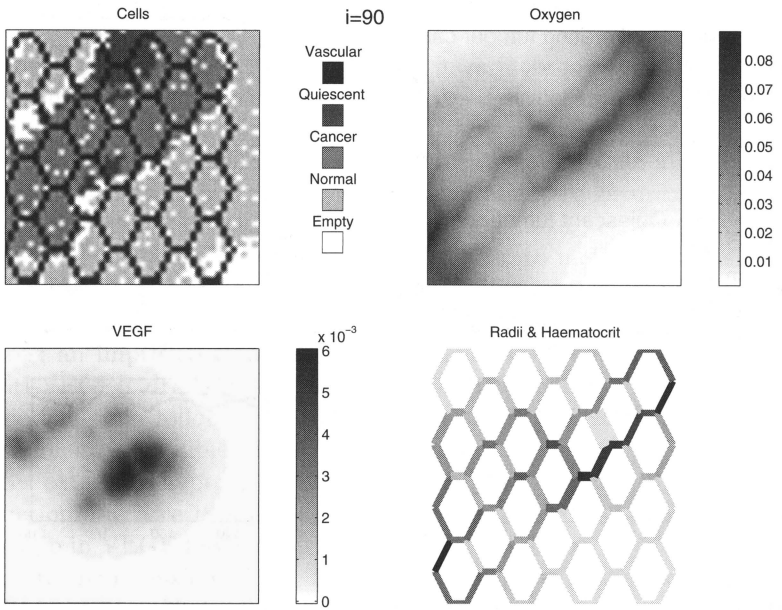

Fig. 17.5. Series of plots showing how the simulation presented in Fig. 17.4 has developed at $t = 90$. The tumour continues to penetrate the tissue region. There are now enough quiescent cells to elicit an angiogenic response. As a result, the vasculature has been remodelled, with blood flow and oxygen supply (haematocrit) being directed primarily towards the tumour mass. Reproduced with permission from [BAOMM].

cept that vascular adaptation was independent of VEGF (as per Fig. 17.3). In both cases, the tumours grow to similar sizes. However, when vascular adaptation is independent of VEGF the evolution is monotonic, the oscillations in the cell populations disappear and the number of quiescent cells is consistently much lower. These results show how coupling between the different spatial scales can effect not only the tumour's growth dynamics but also the proportion of proliferating and quiescent cells that it contains.

Vessel pruning may enhance a tumour's response to radiotherapy

We can use our model to investigate the effects of decreasing the blood vessel number (a primitive way of investigating the effects of anti-angiogenesis treatments). Our results suggest that low levels of vessel pruning may, in certain cases, *enhance* tumour growth by creating a vasculature that allows nutrient to reach tissue more effectively [ABM04b]. It is observed clinically that combination therapy involving anti-angiogenesis treatment and radiotherapy can be more effective than radiotherapy alone and at first glance this seems counter-intuitive. One possible explanation of this observation is provided by

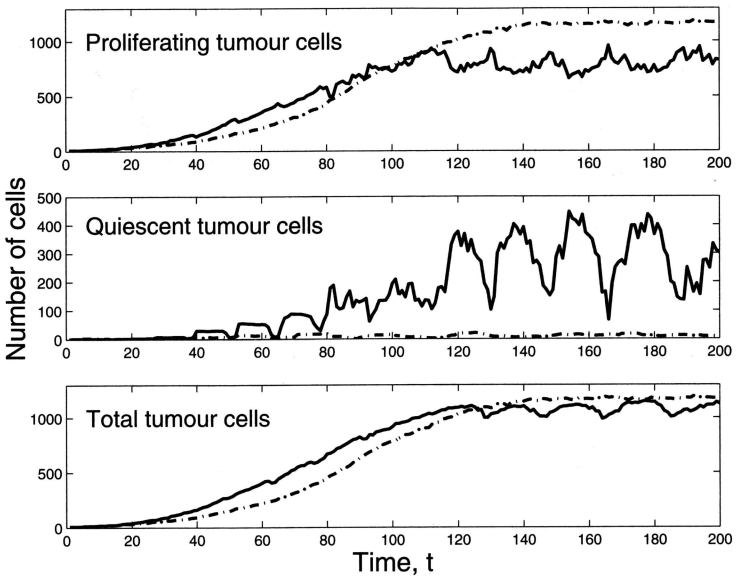

Fig. 17.6. Series of curves showing how, for the simulation in Figs. 17.4 and 17.5, the numbers of proliferating (upper panel), quiescent (middle panel) and total tumour cells (lower panel) change over time. While the number of proliferating cells increases steadily, the number of quiescent cells undergoes oscillations of increasing amplitude until $t \approx 120$. Thereafter, the tumour is sufficiently large that the quiescent cells are never eliminated: quiescent cells that die are replaced by proliferating cells that become quiescent. The dot-dashed lines show the evolution of a tumour which is identical except that its vasculature is not regulated by VEGF. While both tumours reach similar equilibrium sizes, when vascular adaptation is independent of VEGF the oscillations in the cell populations disappear and the number of quiescent cells is much lower. Reproduced with permission from [BAOMM].

the results from our model. An alternative explanation invokes vessel renormalisation [Jain88], and it is now a challenge to the experimental community to devise experiments to distinguish between these possibilities.

Abnormal vascular adaptation alters the tumour's growth dynamics

As mentioned in Section 17.3.1, there is still no good (experimental) model available for vascular adaptation in tumours. It is known, however, that the tumour neovasculature is abnormal in its response mechanisms to signalling cues. Therefore we can use the above model framework to investigate the effects on tumour growth and composition of the failure of different adaptation mechanisms [AOBM06]. This presents the intriguing possibility of being able to determine properties of the vasculature by examination of tumour tissue.

Vessel dematuration reduces the efficacy of chemotherapy

As a further extension of our model, we have incorporated tumour-induced vessel dematuration to assess the effect of vessel structure on the performance of chemotherapeutic agents [RMZAM, AOBM06]. We have found that dematuration can lead to the formation of quiescent regions that are much larger than those observed in simulations with a normal vasculature, thereby hampering the efficacy of cytotoxic drugs designed to target rapidly proliferating (tumour) cells. A further extension has been to include a diffusible anti-VEGFR drug which inhibits the effect of VEGF by competitively binding its receptor [AOBM06]. Our model simulations reproduce two key experimental features: an improved response to cytotoxic drugs following treatment with an anti-VEGFR drug and the emergence of a "window of opportunity," *i.e.* a period of time following treatment with anti-VEGFR during which such improvement is possible. The window opens because the anti-VEGFR drug induces extensive hypoxia within the tumour. This leads to massive VEGF production and a certain amount of cell death caused by oxygen starvation. The surge in VEGF levels stimulates remodelling of the vasculature, bringing oxygen to the hypoxic regions. This effect, coupled with the reduction in oxygen demand caused by cell death there, leads to reoxygenation of the hypoxic regions and a temporary reduction in the size of the quiescent subpopulation. As other regions of the tumour become hypoxic and blood flow undergoes another period of adaptation, the window of opportunity closes.

Explicit incorporation of angiogenesis alters the tumour's growth dynamics

While vessel radii and blood flow within the branches of the vascular network may change over time and, thereby, regulate the supply of nutrients to the tissue, the morphology of the vascular network in the simulations presented above does not change over time. More specifically, the hexagonal symmetry of the network is fixed, angiogenesis is not incorporated explicitly and redundant branches of the network in which blood flow is low do not regress. We have recently modified our model to address these issues [OAMB08], and results from a typical simulation are presented in Fig. 17.7. As the tumour grows and the metabolic demands of the tissue change, VEGF stimulates the ingrowth of new capillary tips towards quiescent regions where VEGF levels are high. Capillary tips that connect successfully to the network alter the morphology of the vasculature and, thereby, alter the pattern of blood flow within, and nutrient supply to, the tissue. As a result of the new connections, the flow through existing vessels may fall and, if low flow (and, hence, low wall shear stress) is maintained for a sufficiently long period, then the vessel is pruned or removed from the system.

For comparison with the basic model, in which angiogenesis is treated implicitly, we present in Fig. 17.8 spatially averaged time-activity curves showing how the coupled dynamics of the tumour and vasculature depend on the way in which vascular adaptation is modelled. The main features to note are the

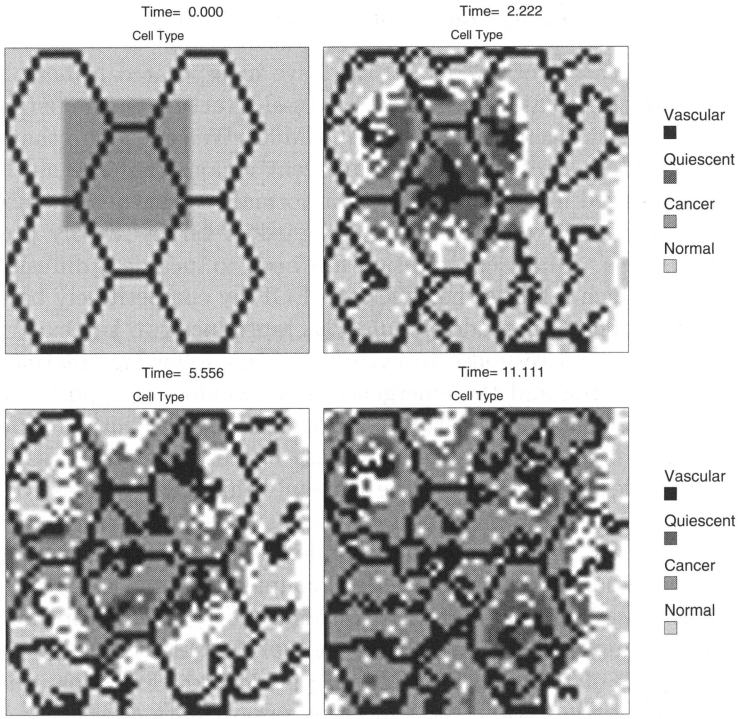

Fig. 17.7. Results from a simulation in which angiogenesis is incorporated explicitly into the vascular remodelling algorithm, thereby allowing the development of arbitrary, asymmetric vascular networks. The plots show the evolution of a small tumour that is embedded, at $t = 0$, into a tissue perfused initially by a hexagonal network of blood vessels. Over time, the structure of the vasculature changes, with existing vessels remodelling and new vessels forming as a result of angiogenesis. The new capillary tips emerge from existing vessels and migrate, via chemotaxis, towards regions of high VEGF concentration. The capillary tips must form connections, and establish a flow, within a fixed period of time; otherwise they regress. The four images show the tissue composition at times $t = 0.00$, $t = 2.22$, $t = 5.55$ and $t = 11.11$.

increase in the number of proliferating tumour cells and the decrease in the number of quiescent tumour cells that occur when angiogenesis is treated explicitly rather than implicitly. These changes are a consequence of the higher spatial resolution that occurs when individual capillary tips are simulated: VEGF produced by quiescent tumour cells will now stimulate the ingrowth of new capillary tips into that region and enable the cells to resume proliferation.

Since our new model distinguishes between blunt-ended capillary tips (in which flow is absent) and vessels which are part of the flow network, it should be possible to generate more detailed predictions concerning the relative efficacy of drugs that target proliferating endothelial cells and those that reduce

blood flow. Additionally, it will be possible to determine whether low levels of chemotherapy targeted at proliferating tumour cells produce an additional beneficial effect by destroying angiogenic tumour vessels and, thereby, reducing the supply of nutrients to the tumour mass [Sha06].

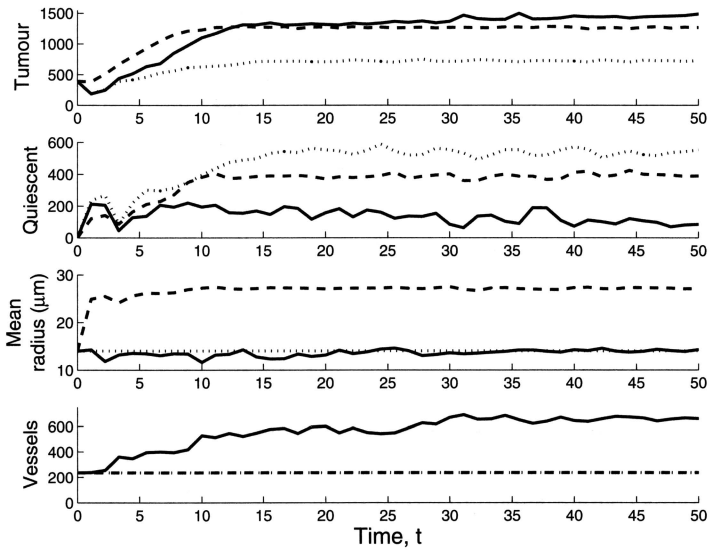

Fig. 17.8. Series of plots showing how the evolution over time of the numbers of proliferating (upper panel) and quiescent (second panel) tumour cells, mean vessel radius (third panel) and number of vessels (lowest panel) depends on the mechanisms that control vascular remodelling. Key: Dotted line, remodelling of the vasculature is independent of VEGF; Dashed line, VEGF enhances vascular remodelling by stimulating vessel dilation; solid line, VEGF enhances vascular remodelling by stimulating angiogenesis.

17.4 Colorectal Cancer

Colorectal cancer (CRC) was the second most commonly diagnosed malignancy in Europe in 2006 [Ferl07]; it also ranked second according to cancer mortality. Most CRCs occur spontaneously, developing from pre-existing, benign polyps (or adenomas), which originate from the epithelial sheet that lines the luminal surface of the bowel. The intestinal epithelium is characterised by numerous invaginations (Fig. 17.9), or crypts, which drive its rapid self-renewal. Near the bottom of the crypts, a small number of stem cells proliferate continuously, producing transit cells, which divide several times before undergoing terminal differentiation. At the same time, cells migrate upwards

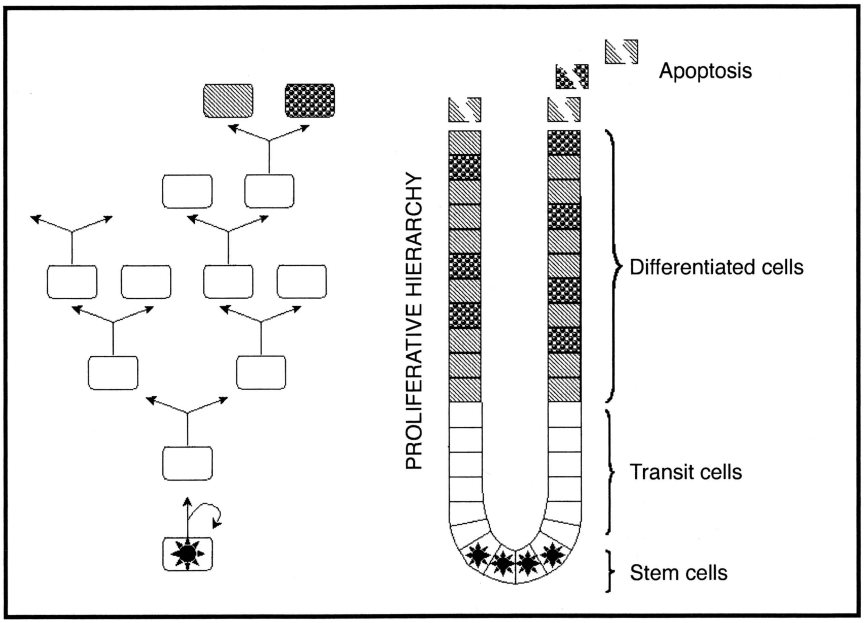

Fig. 17.9. Schematic of the proliferative hierarchy in a normal colonic crypt. Murine crypts contain about 235–250 epithelial cells, which reside on a basement membrane. Proliferating cells (*i.e.* stem and transit cells) occupy the lower third of the crypt. After several divisions, transit cells differentiate into the various cell types that constitute the epithelium (*e.g.* columnar cells and goblet cells).

along the crypt axis and, when they reach the orifice, initiate programmed cell death (apoptosis). Thus a normal crypt can be viewed as a dynamic system in which the processes of cell proliferation, migration, differentiation and death are tightly coordinated by intra-, inter- and extra-cellular cues. Under aberrant conditions genetic and epigenetic alterations cause dysfunctional regulation and loss of homeostasis, eventually leading to the formation of a polyp. Further mutations are required for progression towards a malignant, metastatic carcinoma. Hence, CRC is a multistep, multiscale process in which the progressive accumulation of changes at the molecular level translates into subsequent pathological stages at the macroscale level.

CRC is a natural subject for mathematical investigation because many of the key mutations that arise have been identified and details of their functional effect determined. For example, most CRCs bear inactivating mutations in the *APC* tumour suppressor gene [Ilya05]. This multifunctional protein is a central player in Wingless/Int (Wnt) signalling, a key pathway in the regulation of normal crypt dynamics [Nath04, Sans04]. In the absence of extracellular Wnt, a protein complex that includes Apc marks any free β-catenin molecules for rapid degradation. In contrast, when extracellular Wnt is present, stimulation

of specific receptors on the cell's surface inactivates the Apc-complex and β-catenin accumulates. This protein then travels to the nucleus where it induces the expression of a large number of Wnt targets, including genes involved in cell-cycle control, active migration and differentiation. Genetic alterations detected in CRCs generally impede Apc-mediated β-catenin degradation, and, hence, have the same effect as a continuous Wnt signal.

Since CRC has been extensively studied, it is not surprising that a plethora of mathematical models exist that address various aspects of the disease (for a critical review, see [vLBJK06]). For example, as early as 1954, Armitage and Doll [Armi54] developed a stochastic "time to tumour" model, to describe the observed age-dependent CRC incidence. More recently, Komarova and Wang [Koma04] have investigated the likely targets for malignant transformation in the crypt, while d'Onofrio and Tomlinson [dOno07] and Johnston *et al.* [JEBMC] have analysed the cellular changes that can lead to uncontrolled, exponential growth. We introduce here a series of models that simulate different aspects of the normal gut and CRC. Thereafter, we explain how we are adapting, extending and integrating these models to obtain a detailed, mechanistic multiscale model of CRC [vLEIB, Gava05].

17.4.1 Mathematical Modelling

The earliest models of normal crypt dynamics are formulated on simple two-dimensional (2D) grids (the cylindrical crypt is cut open and rolled out to give a surface), with cells assumed to move within predefined rows and columns [Loef86, Paul93]. All cells have the same, constant (rectangular) shape and size, and cell growth is thus ignored. Proliferation and cell-cycle control are modelled by assigning cell-cycle times to daughter cells immediately after division. Cell movement is driven by mitotic pressure: displacements occur naturally when newborn cells are inserted into the grid. Finally, the rules that govern whether a cell differentiates differ for stem and transit cells. After stem cell division, each daughter cell has a certain probability of leaving the stem cell pool and becoming a transit cell. In contrast, transit cells differentiate terminally after a fixed number of divisions. In summary, the 2D grid models can be viewed as basic multiscale models: a 2D tissue is characterised by the behaviour of its cellular constituents, each of which carries its own subcellular cell-cycle time and a record of its differentiation status.

Despite their simplicity, 2D grid models have been successfully used to interpret experimental data concerning cell migration and differentiation in the crypt [Loef86, Paul93]. The main drawback with the 2D approach is that the insertion of newborn cells inevitably shifts a whole column of cells upwards, breaking many cell-cell contacts. This is physically unrealistic as epithelial cells are known to have strong cell-cell connections so that they may form a protective barrier between the body and the contents of the gut. To overcome this deficiency, Meineke *et al.* [Mein01] proposed a 2D lattice-free model in which cell centres are represented as points that can occupy any position on a

2D surface with cylindrical boundary conditions. Polygonal cell shapes, which resemble real epithelial cells, are then determined from the associated Voronoi diagram while cell-cycle control and differentiation are incorporated as in the 2D grid models. Migration and cell-cell adhesion are accounted for by assuming that neighbouring cells are connected by damped springs and balancing the forces due to the spring connections with damping forces associated with cell-substrate binding (see Fig. 17.10). Hence, the position vector x_i for cell i at time $t + \triangle t$ is determined from its position and that of its neighbours at time t as follows:

$$x_i(t + \triangle t) = x_i(t) + \frac{\mu}{\eta} \sum_{\forall j} u_{ij}(t)(d_{ij}(t) - L_{ij}(t))\triangle t, \tag{17.2}$$

where the summation is over all cells connected to cell i at time t, u_{ij} is a unit vector pointing from cell i to j, L_{ij} is the equilibrium spring length, d_{ij} the distance between i and j, μ the spring constant, and η the damping constant. In contrast to the 2D grid models, cell division now results in local cell rearrangements only.

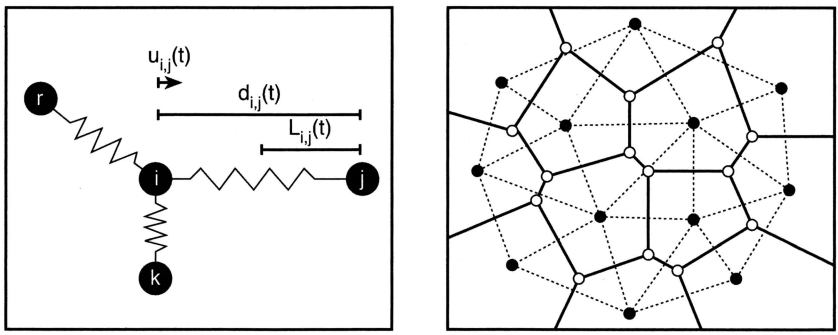

Fig. 17.10. Schematics illustrating the lattice-free approach developed in [Mein01]. (Left) *In silico* cells attached by springs. (Right) *In silico* 2D tissue, showing cell centres (black nodes), vertices (white nodes) and the associated Voronoi tesselation (solid lines). The related Delauney triangulation (dashed lines) is obtained by connecting all neighbouring nodes and defines the network of springs. Reproduced with permission from [vLEIB].

17.4.2 Multiscale Model Assembly

The spatial models described above do not account for subcellular pathways and are, therefore, unable to predict the impact of specific genetic alterations (*e.g.* mutations in the Wnt network) on crypt dynamics. Nor can they be used to explore potential interactions between phenomena occurring at different levels of organisation or to evaluate the impact of cancer drugs on the

system. These aims can be achieved by developing a multiscale framework (see Fig. 17.11) that embraces each level of organisation, from molecule to whole organ, in a manner similar to that used to formulate the multiscale model of vascular tumour growth presented in Section 17.3. Building such a framework, and coupling models developed originally to describe phenomena at a single scale, raises many mathematical challenges, four of which we highlight below.

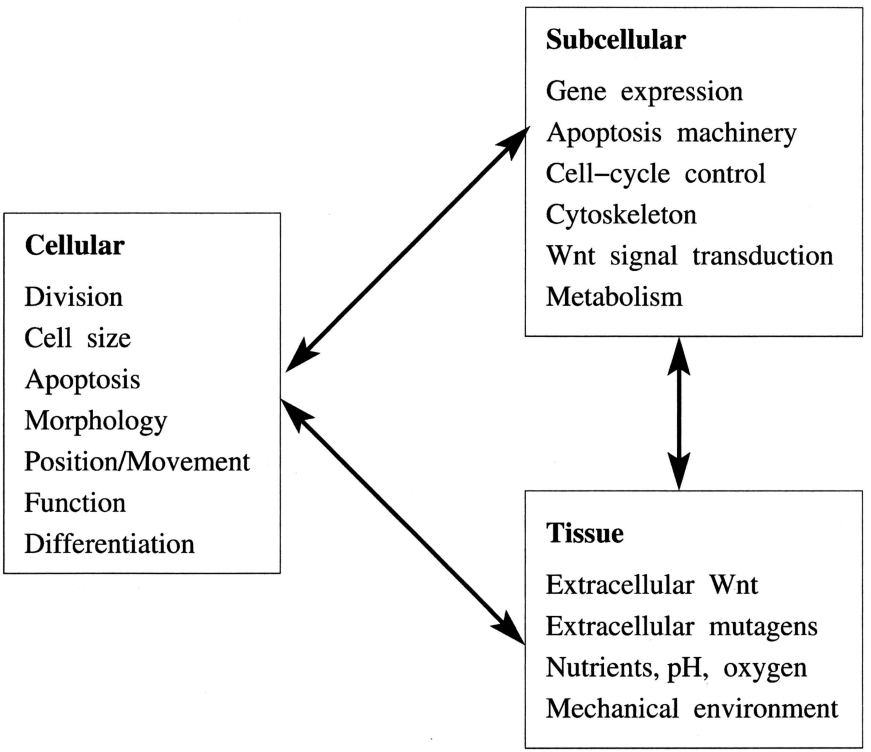

Fig. 17.11. Prototype multiscale model for normal crypt dynamics and CRC. The arrows highlight that the relation between the scales is not simply bottom-up. An extracellular, tissue gradient of Wnt factors, for example, can directly affect subcellular gene expression.

Incorporating extracellular signalling

In the basic model developed in [Mein01] all cellular processes are assumed to be independent of extra- and intra-cellular signals. Experimental evidence suggests, however, that epithelial cells respond to spatial variations in: the composition of the basement membrane; the signals emitted by myofibroblasts; and the level of Wnt factors. By imposing an extracellular Wnt gradient along

the vertical crypt axis and using simple models of the (intracellular) Wnt signalling pathway [Lee03, vLBJK07] we are able to predict position-dependent patterns of gene expression. Coupling the Wnt-signalling model with a cell-cycle model (*e.g.* [Swat04, TN01]) provides additional information about how cell-cycle times vary along the crypt axis and how terminally differentiated (*i.e.* non-cycling) cells are generated.

Controlling cell size

In the 2D grid models cell sizes are fixed, whereas in [Mein01] cell size is controlled by the relative spatial position of neighbouring cells. In reality, however, cell size depends on nutrient availability, the cell's metabolic rate, its progress through the cell cycle and contact inhibition. Better control of cell growth and size is thus needed. Cell vertex models, for instance, achieve this goal by associating with the system an energy function which increases as cells deviate from their optimal sizes [Brod04]. Cells are assumed to move in directions that minimise the energy function.

Including cell death

In existing models cell removal occurs only when cells are pushed off the upper edge of the 2D surface. Apoptosis can, however, occur within the crypt at rates which are enhanced by certain experimental manipulations, such as Apc knockout [Sans04] and irradiation [Pott94]. To simulate and explain these results, our model must account for biochemical networks that regulate programmed cell death, biomechanical cell detachment and the resulting changes at the cellular level. At the macroscale, this poses the additional problem of dealing with gaps in the tissue.

Modelling domain growth

In the models described above, the 2D surface remains fixed during the simulation period. Although this may be a good approximation for normal crypts, a more flexible approach is required to describe the changes in crypt size and morphology associated with aberrant crypts and polyp formation. The model of morphogenesis and crypt fission developed in [Dras01] provides one possible resolution to this problem. In [Dras01] Drasdo and Loeffler consider a 1D longitudinal section of a crypt, represent individual cells as deformable circles and assume that migration is driven by cell division. Alternatively, the continuum model of crypt fission developed by Edwards and Chapman [Edwa07] could be adapted to allow for changes in crypt size caused by genetic mutations. In [Edwa07] the epithelial cells are treated as a continuous tissue layer that is attached to a basement membrane by viscoelastic bonds. Model simulations suggest that mutations causing either a net increase in cell proliferation or an increase in the strength of cell bonding can lead to buckling and fission.

17.5 Discussion

We have presented a series of multiscale models of cancer growth, focused on carcinogenesis in early ductal carcinoma *in situ*, vascular tumour growth and colorectal cancer. While we have focused on three particular applications, it is important to note that this is a rapidly growing area of research. For example, Jiang *et al.* [JPCF] have formulated a multicellular model to simulate the growth of multicellular tumour spheroids, using a discrete lattice Monte Carlo model to describe the cellular dynamics and a Boolean network to model the expression of proteins that control the cell cycle. Equally, Patel *et al.* [PGLG] have developed a model for early tumour growth and metabolism that considers the interaction of native tumour vascularity and increased glycolysis. Anderson and colleagues [AWCQ06, GA07] have investigated the effects of heterogeneity in the tissue and nutrient levels on the dynamics of tumour growth and have combined this with mutation and evolution to show mechanisms whereby the classical fingering morphology of a tumour can arise and how the microenvironment can select certain genotypes. Macklin and Lowengrub [ML07] have focused on the biomechanical aspects of a growing tumour mass to predict fingering as a result of microenvironmental factors. Ribba *et al.* [RCS06] have developed a model for colorectal oncogenesis which includes a Boolean description of a genetic model, integrated with a discrete model of the cell cycle and a continuous macroscopic model of tumour growth and invasion. They have used this model to predict the effects of radiotherapy.

While considerable progress has been made in a very short time, many challenges remain ahead. For example, it is impossible (and not desirable) to have a detailed comprehensive model of every process involved in tumour growth. Simplifications need to be made. In modelling a process at one specific spatial scale, we have well-established techniques for determining the errors incurred in making such simplifications. However, when we couple such models into an integrated framework spanning several spatial scales with multiple feedback, as well as feedforward, loops, we have little idea of how errors propagate and grow: to understand this is a huge challenge for the future.

The multiscale approaches outlined in this paper appear to be the natural framework for modelling in this area, but they quickly become computationally infeasible as we try to model a growing tumour consisting of billions of cells. For that we need a continuum approach, but it is not clear how to interface between discrete models (appropriate for small cell numbers) and continuous models, appropriate for large-scale models.

Biological systems are highly robust and therefore we would expect the behaviour of the system to be insensitive to many parameters but crucially dependent on a few select parameters. Therefore, for modelling we may only need crude estimates for most parameters. Model simulations can be performed to identify those parameters to which the system dynamics are most sensitive and thus direct experimental effort to focus on accurate measurements of these parameters. To be successful it is therefore vital that model

development be undertaken in close collaboration with experimentalists, and that experimental design and data collection pay attention to the needs of models.

Acknowledgments

PKM was partially supported by a Royal Society-Wolfson Merit Award and NIH grant U56CA113004 from the National Cancer Institute. TA and IMMvL gratefully acknowledge the EPSRC for financial support.

References

[Ad96] Adam, J.A.: Mathematical models of perivascular spheriod development and catastrophe-theoretic description of rapid metastatic growth/tumor remission, Invasion Metastasis, **16**, 247–267 (1996).

[ABM03] Alarcón, T., Byrne, H.M., and Maini, P.K.: A cellular automaton model for tumour growth in inhomogeneous environment, J. Theor. Biol., **225**, 257–274 (2003).

[ABM04b] Alarcón, T., Byrne, H.M., and Maini, P.K.: Towards whole-organ modelling of tumour growth, Prog. Biophys. Mol. Biol., **85**, 451–472 (2004).

[ABM05a] Alarcón, T., Byrne, H.M., and Maini, P.K.: A multiple scale model for tumour growth, Multiscale Mod. Sim., **3**, 440–475 (2005).

[ABM05b] Alarcón, T., Byrne, H.M., and Maini, P.K.: A design principle for vascular beds: the effects of complex blood rheology, Microvasc. Res., **69**, 156–172 (2005).

[AOBM06] Alarcón, T., Owen, M.R., Byrne, H.M., and Maini, P.K.: Multiscale modelling of tumour growth and therapy: the influence of vessel normalisation on chemotherapy, Comp. Math. Methods Med., **7**, 85–119 (2006).

[AC98] Anderson, A.R.A., and Chaplain, M.A.J.: Continuous and discrete mathematical models of tumour-induced angiogenesis, Bull. Math. Biol., **60**, 857–899 (1998).

[AWCQ06] Anderson, A.R.A., Weaver, A.M., Cummings, T.M., and Quaranta, V.: Tumor morphology and phenotypic evolution driven by selective pressure from the microenvironment, Cell, **127**, 905–915 (2006).

[AMcE] Araujo, R.P., and McElwain, D.L.S.: A history of the study of solid tumor growth: the contribution of mathematical modelling, Bull. Math. Biol., **66**, 1039–1091 (2004).

[Armi54] Armitage, P., and Doll, R.: The age distribution of cancer and a multistage theory of carcinogenesis, Br. J. Cancer, **8**, 1–12 (1954).

[Brod04] Brodland, G.W.: Computational modeling of cell sorting, tissue engulfment, and related phenomena: a review, Appl. Mech. Rev., **57**, 47–76 (2004).

[BAOMM] Byrne, H.M., Alarcón, T., Owen, M.R., Murphy, J., and Maini, P.K.: Modelling the response of vascular tumours to chemotherapy: a multiscale approach, Math. Mod. Meth. Appl. Sci., **16**, 1219–1241 Suppl S (2006).

[Cram04] Crampin, E.J., Halstead, M., Hunter, P., Nielsen, P., Noble, D., Smith, N., and Tawhai, M.: Computational physiology and the Physiome project, Exp. Physiol., **89**, 21–26 (2004).

[Dras01] Drasdo, D., and Loeffler, M.: Individual-based models to growth and folding in one-layered tissues: intestinal crypts and early development, Nonlinear Analysis, **47**, 245–256 (2001).

[Edwa07] Edwards, C.M., and Chapman, J.S.: Biomechanical modelling of colorectal crypt budding and fission, Bull. Math. Biol., **69**, 1927–1942, (2007).

[Ferl07] Ferlay, F., Autier, P., Boniol, M., Heanue, M., Colombet, M., and Boyle, P.: Estimates of the cancer incidence and mortality in Europe in 2006, Ann. Oncol., **18**, 581–592 (2007).

[F93] Fung, Y.C.: Biomechanics, Springer, New York (1993).

[GG96] Gatenby, R.A., and Gawlinski, E.T.: A reaction-diffusion model of cancer invasion, Cancer Res., **56**, 5745–5753 (1996).

[GG04] Gatenby, R.A., and Gillies, R.J.: Why do cancers have high aerobic glycolysis? Nature Rev. Cancer, **4**, 891–899 (2004).

[GM03] Gatenby, R.A., and Maini, P.K.: Mathematical oncology: cancer summed up, Nature, **421**, 321 (2003).

[GS07] Gatenby, R.A., Smallbone, K., Maini, P.K., Rose, F., Averill, J., Nagel, R.B., Worrall, L., and Gillies, R.J.: Cellular adaptations to hypoxia and acidosis during somatic evolution of breast cancer, Brit. J. Cancer, **97**, 646–653 (2007).

[Gava05] Gavaghan, D.J., Simpson, A.C., Lloyd, S., MacRandal, D.F., and Boyd, D.R.: Towards a Grid infrastructure to support integrative approaches to biological research, Philos. Transact. A Math. Phys. Eng. Sci., **363**, 1829–1841 (2005).

[GA07] Gerlee, P., and Anderson, A.R.A.: An evolutionary hybrid cellular automaton model of solid tumour growth, J. Theor. Biol., **246**, 583–603 (2007).

[GLB94] Gillies, R.J., Liu, Z., and Bhujwalla, Z.: ^{31}P-MRS measurements of extracellular pH of tumors using 3-aminopropylphosphonate, Am. J. Physiol., **267**, 195–203 (1994).

[GRM89] Grinstein, S., Rotin, D., and Mason, M.J.: Na^+/H^+ exchange and growth factor-induced cytosolic pH changes: role in cellular proliferation, Biochim. Biophys. Acta, **988**, 73–97 (1989).

[HSR91] Haberkorn, U., Strauss, L.G., Reisser, C., Hagg, D., Dimitrakopoulu, A., Ziegler, S., Oberdorfe, F., Rudat, V., and van Kaick, G.: Glucose uptake, perfusion, and cell proliferation in head and neck tumours: relation to positron emission tomography and other whole-body applications, Semin. Nuc. Med., **22**, 268–284 (1991).

[HW00] Hanahan, D., and Weinberg, R.A.: The hallmarks of cancer, Cell, **100**, 57–70 (2000).

[Ilya05] Ilyas, M.: Wnt signalling and the mechanistic basis of tumour development, J. Pathol., **205**, 130–144 (2005).

[Jain88] Jain, R.K.: Determinants of tumour blood flow: a review, Cancer Res., **48**, 2641–2658 (1988).

[JPCF] Jiang, Y., Pjseivac-Grbovic, J., Cantrell, C., and Freyer, J.P.: A multiscale model for avascular tumour growth, Biophys. J., **89**, 3884–3894 (2005).

[JEBMC] Johnston, M.D., Edwards, C.M., Bodmer, W.F., Maini, P.K., and Chapman, S.J.: Mathematical modelling of cell population dynamics in the colonic crypt, Proc. Natl. Acad. Sci., **104**, 4008–4013 (2007).

[Koma04] Komarova, N.L., and Wang, L.: Initiation of colorectal cancer: where do the two hits hit?, Cell Cycle, **3**, 1558–1565 (2004).

[Lee03] Lee, E., Salic, A., Kruger, R., Heinrich, R., and Kirschner, M.W.: The roles of APC and Axin derived from experimental and theoretical analysis of the Wnt pathway, PLoS Biol., **1**, E10 (2003).

[vLBJK06] van Leeuwen, I.M.M., Byrne, H.M., Jensen, O.E., and King, J.R.: Crypt dynamics and colorectal cancer: advances in mathematical modelling, Cell Prolif., **39**, 157–181 (2006).

[vLBJK07] van Leeuwen, I.M.M., Byrne, H.M., Jensen, O.E., and King, J.R.: Elucidating the interactions between the adhesive and transcriptional functions of beta-catenin in normal and cancerous cells, J. Theor. Biol., **247**, 77–102 (2007).

[vLEIB] van Leeuwen, I.M.M., Edwards, C.M., Ilyas, M., and Byrne, H.M.: Towards a multiscale model of colorectal cancer, W. J. Gastroenterol., **13**, 1399–1407 (2007).

[Loef86] Loeffler, M., Stein, R., Wichmann, H.E., Potten, C.S., Kaur, P., and Chwalinski, S.: Intestinal crypt proliferation. I. A comprehensive model of steady-state proliferation in the crypt, Cell Tissue Kinetics, **19**, 627–645 (1986).

[MACS02] McDougall, S.R., Anderson, A.R.A., Chaplain, M.A.J., and Sherratt, J.A.: Mathematical modelling of flow through vascular networks: implications for tumour-induced angiogenesis and chemotherapy strategies, Bull. Math. Biol., **64**, 673–702 (2002).

[MAC06] McDougall, S.R., Anderson, A.R.A., and Chaplain, M.A.J.: Mathematical modelling of dynamic adaptive tumour-induced angiogenesis: clinical implications and therapeutic targeting strategies. Bull. Math. Biol., **241**, 564–589 (2006).

[ML07] Macklin, P., and Lowengrub, J.: Nonlinear simulation of the effect of microenvironment on tumor growth, J. Theor. Biol., **245**, 677–704 (2007).

[Mein01] Meineke, F.A., Potten, C.S., and Loeffler, M.: Cell migration and organization in the intestinal crypt using a lattice-free model, Cell Prolif., **34**, 253–266 (2001).

[Nath04] Näthke, I.S.: The adenomatous polyposis coli protein: the Achilles heel of the gut epithelium, Annu. Rev. Dev. Biol., **20**, 337–366 (2004).

[Nobl06] Noble, D.: Systems biology and the heart, Biosystems, **83**, 75–80 (2005).

[dOno07] d'Onofrio, A., and Tomlinson, I.P.: A nonlinear mathematical model of cell turnover, differentiation and tumorigenesis in the intestinal crypt, J. Theor. Biol., **244**, 367–374 (2007).

[OAMB08] Owen, M.R., Alarcón, T., Maini, P.K., and Byrne, H.M.: Angiogenesis and vascular remodelling in normal and cancerous tissues, J. Math. Biol., in press.

[Pan97] Panetta, J.C.: A mathematical model of breast and ovarian cancer treated with paclitaxel, Math. Biosci., **146**, 89–113 (1997).

[PGLG] Patel, A.A., Gawlinsky, E.T., Lemieux, S.K., and Gatenby, R.A.: Cellular automaton model of early tumour growth and invasion: the effects of native tissue vascularity and increased anaerobic tumour metabolism, J. Theor. Biol., **213**, 315–331 (2001).

[Paul93] Paulus, U., Loeffler, M., Zeidler, J., Owen, G., and Potten, C.S.: The differentiation and lineage development of goblet cells in the murine small intestinal crypt: experimental and modelling studies, J. Cell Sci., **106**, 473–484 (1993).

[Pott94] Potten, C.S., Merritt, A., Hickman, J., Hall, P., and Faranda, A.: Characterization of radiation-induced apoptosis in the small intestine and its biological implications, Int. J. Radiat. Biol., **65**, 71–78 (1994).

[PSG98] Pries, A.R., Secomb, T.W., and Gaehtgens, P.: Structural adaptation and stability of microvascular networks: theory and simulations, Am. J. Physiol., **275**, H349–H360 (1998).

[RMZAM] Ribba, B., Marron, K., Agur, Z., Alarcón, T., and Maini, P.K.: A mathematical model of doxorubicin treatment efficacy for non-Hodgkin's lymphoma: investigation of the current protocol through theoretical modelling results, Bull. Math. Biol., **67**, 79–99 (2005).

[RCS06] Ribba, B., Colin, T., and Schnell, S.: A multiscale mathematical model of cancer and its use in analyzing irradiation therapies, Theor. Biol. Med. Model., **3**, 7 (2006).

[RCM07] Roose, T., Chapman, S.J., and Maini, P.K.: Mathematical models of avascular tumour growth, SIAM Review, **49**, 179–208 (2007).

[Sans04] Sansom, O.J., Reed, K.R., Hayes, A.J., Ireland, H., Brinkmann, H., Newton, I.P., Batlle, E., Simon-Assman, P., Clevers, H., Nathke, I.S., Clarke, A.R., and Winton, D.J.: Loss of Apc *in vivo* immediately perturbs Wnt signaling, differentiation, and migration, Genes Dev, **18**, 1385–1390 (2004).

[Sha06] Shaked, Y., Ciarrocchi, A., Franco, M., Lee, C.R., Man, S., Cheung, A.M., Kicklin, D.J., Chaplin, D., Foster, F.S., Benezra, R., and Kerbel, R.S.: Therapy-induced acute recruitment of circulating endothelial progenitor cells to tumours. Science, **313**, 1785–1787 (2006).

[SGGMG07] Smallbone, K., Gatenby, R.A., Gillies, R.J., Maini, P.K., and Gavaghan, D.J.: Metabolic changes during carcinogenesis: potential impact on invasiveness. J. Theor. Biol., **244**, 703–713 (2007).

[Swat04] Swat, M., Kel, A., and Herzel, H.: Bifurcation analysis of the regulatory modules of the mammalian G_1/S transition, Bioinformatics, **20**, 1506–1511 (2004).

[TN01] Tyson, J.J., and Novak, B.: Regulation of the eukariotic cell-cycle: molecular anatagonism, hysteresis, and irreversible transitions, J. Theor. Biol., **210**, 249–263 (2001).

[W30] Warburg, O.: The Metabolism of Tumours, Constable Press, London (1930).